Structure evolution of manganese stabilized zirconia

LING GAO[a,b], LIAN ZHOU[b], CHENGSHAN LI[b], JIANQING FENG[b], YAFENG LU[b,*]
[a]*Institute of Materials and Metallurgy, Northeastern University, Shenyang, Liaoning 110004, P. R. China*
[b]*Northwest Institute for Nonferrous Metal Research, P.O. Box 51, Xi'an, Shaanxi 710016, P. R. China*

Structural development was systematically studied in $Zr_{1-x}Mn_xO_{2-\delta}$(x = 0~0.5) prepared at the sintering temperature of 1400℃ in Ar for 12h. It is found that the Mn ions go into the crystal lattice of ZrO_2 to form a solid solution without any other compounds formed. After post treatment in high oxygen partial pressure, the cubic phase transforms into the monoclinic phase. We believe that the high symmetry phase can be retained to room temperature due to the effects of vacancy compensation and lattice distortion.

(Received December 15, 2011; accepted February 20, 2012)

Keywords: Oxides, Phase transformations, Microstructure

1. Introduction

Zirconia (ZrO_2) as a kind of new-fashioned structural and functional ceramics attracts many researchers' attentions because of its interesting mechanical properties and physical properties. The pure zirconia has three polymorphic phases: monoclinic (T<1170℃), tetragonal (1170℃<T< 2370℃) and cubic (T>2370℃). But when cooling at 950℃, the zirconia displaces tetragonal to monoclinic phase transformation, accompanied by a shear strain of ~ 0.16 and a volume expansion of ~ 4%. Introduction of cations with valences less than 4 creates a high concentration of oxygen defects which could stabilize the high temperature structure phases to room temperature. The structural developments of ZrO_2 introducing of trivalent or divalent such as Y^{3+}, Ca^{2+} and Mg^{2+} have been investigated extensively [1–3]. However, the details of ZrO_2 stabilized with MnO_x, are still elusive, especially about the valence state of Mn and the solid solution ranges. This system has several points of interest, especially in that the oxygen ions in the zirconia structure have a rather high mobility and their redox properties various with the valence state of Mn. Moreover, in recent theoretical calculation [4], it was predicted that the transition metal doped zirconia might have semi-metallic properties even at room temperature, when the doping ions are at a certain concentration and oxidation state.

In the 1990th', the manganese oxide-zirconium oxide solid solution was reported as a new class of catalysts, which has been widely investigated [5–7]. M. Hino [8] found that the catalysis activity of tetragonal-ZrO_2 (t-ZrO_2) is higher for some catalytic reactions. But for the complete oxidation reaction of hydrocarbon, the cubic ZrO_2 (c-ZrO_2) is usually used [6, 7]. Also, Bell [9] pointed that the activity of monoclinic-ZrO_2 (m-ZrO_2) is higher than t-ZrO_2 for the synthetic carbinol reaction with CO/H_2, CO_2/H_2. In recent years, spintronics has been one of the most important fields for research and engineering. Mn-, Fe- and Co-stabilized zirconia has been reported to be a room-temperature single-spin injector according to the *ab inition* study [4]. Lots of experiments have been done on the cubic-zirconia doping with different concentration of Mn to verify the theoretical calculation by several research groups [10–12]. However, most of them found these systems were absence of ferromagnetism.

As mentioned above, it is clear that the structure of zirconia solid solution is one of the most important factors which can affect its physical properties. In this paper, we present a solid state reaction synthesis Mn-doped ZrO_2 bulk that are doped with up to 50 at.% Mn. The work presented here was undertaken to determine the relationship between the structure of the zirconia solution and the concentration of doping cation ions. We also attempted to study the stability of the cubic phase at various temperatures. These results can be applied to the study of stabilization mechanism, electrical conductivity and magnetic performance.

2. Experiment

Conventional solid state reaction in Ar was used to prepare $Zr_{1-x}Mn_xO_{2-\delta}$ (x = 0~0.5) bulks. Starting materials for the studies were ZrO_2 (SCRC, particle size: 2 ~ 4μm, purity: 99%) and MnO_2 (Alfa Aesar, particle size: 2 ~ 4μm, purity: 99.5%). A proper amount of these powders were mixed in an agate mortar and the powder mixtures were uniaxially pressed into disks by applying a pressure of 10 MPa with the help of a hydraulic press. Then they were sintered at 1400℃ for 12 h in Ar with furnace cooling.

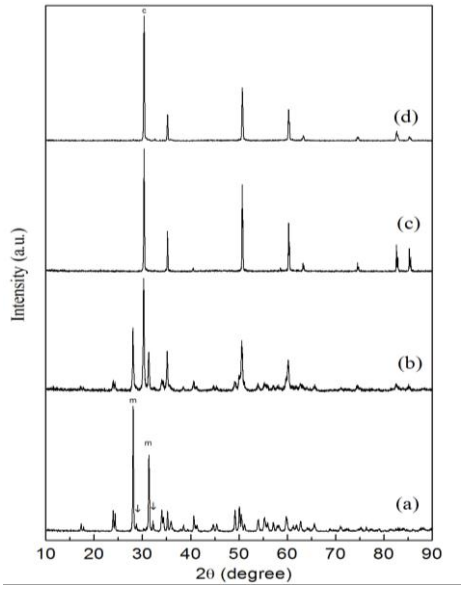

Fig. 1. X-ray diffraction spectra of $Zr_{0.75}Mn_{0.25}O_{2-\delta}$ sintered at (a) 1100 ℃, (b) 1200 ℃, (c) 1300 ℃ and (d) 1400 ℃. c, cubic reflections, m, monoclinic reflections, ↓, Mn_3O_4 reflections.

SEM (JEOL JEM-6460) was used to study the microstructure. Samples were ground with serious grades abrasive paper and polished with canvas, and then the polished samples were thermal etched at 50℃ below the sintering temperature. XRD (Rigaku D/max-2550) with Cu-Kα radiation was used to identify phase composition and determine lattice parameters of the cell. The XRD patterns were recorded in the 2θ range of 10° to 90° . TG-DTA (NETZSCH STA 409) performed to estimate the oxygen deficiency. High-resolution microscopy was performed with a CM200FEG microscope operating at 200 kV and equipped with a field-emission gun. Samples were prepared by ground to a thickness of ~70μm and finally ion milled to impart electron transparency.

3. Results and discussion

So far as we know, the most important influencing factors for the solid state reaction are the reaction temperature and the particle size of the reactive materials. In general, if the reaction temperature is higher, the speed of the reaction is faster. In the Mn-Zr-O system, no ternary compounds or complex manganese zirconium oxides have been reported. So it is much easier for us to distinguish the structures between zirconia solid solution and manganese oxides. A nominal composition of $Zr_{0.75}Mn_{0.25}O_{2-\delta}$ was selected to investigate the influence of sintering temperature on the phase formation. The XRD patterns of the $Zr_{0.75}Mn_{0.25}O_{2-\delta}$ recorded as a function of temperature from 1100℃ to 1400℃ in Ar are given in Fig.1. The sample sintered at 1100 ℃ shows essentially the monoclinic form with some Mn_3O_4 residue. It means that the high-temperature phases are difficult to be gained at room temperature. With increasing the sintering temperature, some diffraction reflections of the high temperature phase were detected. When the sintering temperature is higher than 1300℃, the single cubic phase is formed with some manganese oxides residue. So that 1400℃ was the temperature choice for us to prepare the samples.

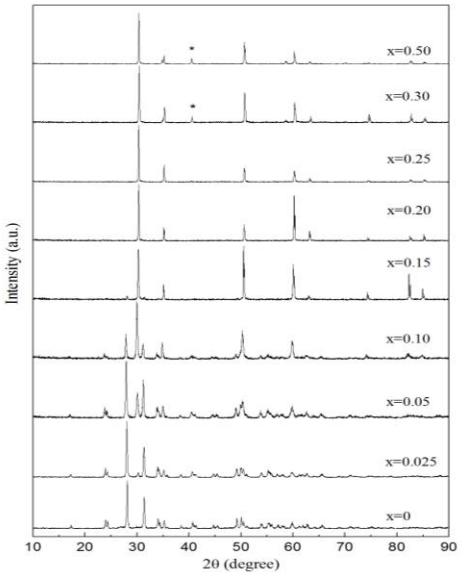

*Fig. 2. XRD patterns of $Zr_{1-x}Mn_xO_{2-\delta}$ with different dopant concentrations sintered at 1400 ℃. *, MnO reflections.*

The XRD patterns of the $Zr_{1-x}Mn_xO_{2-\delta}$ (x = 0 ~ 0.5) at room temperature are shown in Fig. 2. It is possible to see that the samples sintered at 1400℃ undergo a phase transition with increasing the concentration of Mn. When the concentration of Mn is lower than 15 at.%, the monoclinic and cubic phases coexist. The samples doped with up to 20 at.% exhibit only diffraction peaks of the cubic structure, but trance amount of MnO as a second phase is found in the samples with the Mn concentration higher than 30 at.%. Because the (400) reflection is sensitive to the difference between the tetragonal and cubic phases, the diffraction profiles at 2θ = 72 ~ 76° were studied carefully. Peak splitting of the (400) reflection was not found for all the samples. It means that at current reaction conditions, the high symmetry phase is cubic zirconia. The relationship between lattice parameters and structure variation will be discussed later.

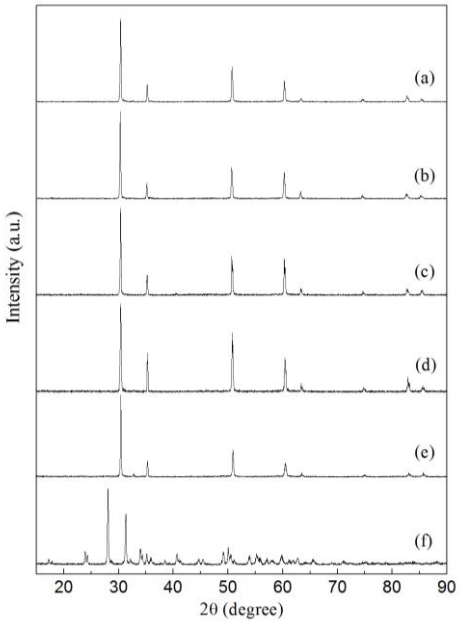

Fig. 3. XRD patterns for (a) as-synthesized $Zr_{0.75}Mn_{0.25}O_{2-\delta}$ solid solution and after annealing in air at the temperature of 200 ℃ (b), 400 ℃ (c), 600 ℃ (d), 800 ℃ (e) and 1000 ℃ (f).

Many researchers found that the so-called cubic zirconia is destabilized by long heat treatment between 1050℃ and 1300℃ and the monoclinic ZrO_2 resolves [14]. Especially for the zirconia solid electrolyte, the stabilization of the cubic crystal structure should be in a large temperature range either in oxidizing or reducing atmosphere. Fig. 3 is XRD patterns of $Zr_{0.75}Mn_{0.25}O_{2-\delta}$ annealed at various temperatures for 6h in air. Fig. 3(a) ~ (e) indicate that the cubic structure is stable below 800℃. When annealed at 900℃, a little of the cubic phase transforms into monoclinic, and if annealing temperature reaches 1000℃, the cubic structure completely changes into monoclinic with some Mn_2O_3 residual. This temperature region of 900 ~ 1000 ℃ is near the destructive monoclinic - tetragonal inversion. The SEM images of the annealed samples (not shown here) show some porosity and cracks. This is due to the decreasing of the oxygen vacancies and the expansion of the crystal cell volume.

The ZrO_2 and MnO_2 mixture with the nominal composition of 20 at.% of MnO_2 and the sintered $Zr_{0.8}Mn_{0.2}O_{2-\delta}$samples were investigated by thermal analysis (TG-DTA) in Ar and air (Fig. 4) individually. Fig. 4(a) refers to the solid state reaction between ZrO_2 and MnO_2 in an Ar atmosphere. Two sharp decreases in mass were observed near 550℃ and 800℃ and very little mass loss was found for higher temperature. According to the literature, the DTA curve reveals two exothermic peaks. Because the pure m-ZrO_2 does not have any thermal effect in this temperature range, it can be concluded that this two peaks correspond to the valance change of Mn. The scatter of the measured decomposition temperature of MnO_2 is very large from 694 to 943 K [15, 16]. The measured decomposition temperature of Mn_2O_3 is from 958 K to 1243 K [17, 18]. Our testing results are within these two ranges. With calculating the loss weight of these two steps, it can be confirmed that the mass loss at 550℃ indicates the MnO_2 decomposition into Mn_2O_3 and O_2 and the mass loss at 800℃ represents the Mn_2O_3 decomposition into Mn_3O_4 and O_2. By using TG-DTA to investigate pure MnO_2 decomposition, Bayer found that MnO formed between 1200 and 1280℃ in N_2 [14]. This reaction was not found in our test and this may be due to the solid state reaction beginning near this temperature range. However, for the high dopant concentration (such as 30 and 50 at.%), some MnO residual was found in Fig. 2 as marked by the star. Although this reaction was not found in this experiment, the detail of this condition will be discussed elsewhere.

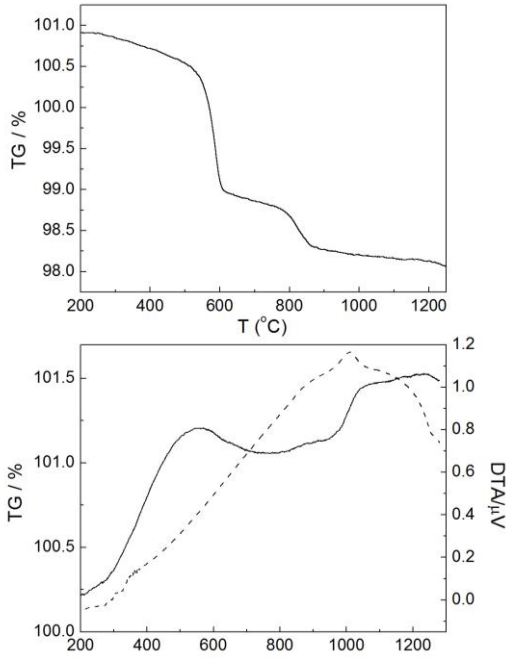

Fig. 4. Thermal gravity (TG) plot of ZrO_2 and MnO_2 mixture in Ar (a) and TG-DTA of $Zr_{0.8}Mn_{0.2}O_{2-\delta}$in air. The solid line is guide for the TG curve and dotted line is for DSC.

Fig. 4(b) shows the TG and DTA curves of the as-synthesized cubic $Zr_{0.8}Mn_{0.2}O_{2-\delta}$ sample during heating in air. With increasing the temperature, two sharp mass increase steps were found at the range from 300℃ to 500℃ and around 1000℃. Unlike the Mn-stabilized HfO_2 [19], there is only one exothermic peak in the heating temperature range up to 1250℃. Comparing with the XRD of the annealing samples at different temperatures (Fig. 3f), the exothermic peak indicates the phase transition from cubic to monoclinic. At the meantime, a mass increase was observed from the TG curve. The oxygen vacancies are reported to be one of the most important effects which can make the high symmetry phase retain to temperature [1]. The number of oxygen vacancy in m-ZrO_2 is smaller than in cubic ZrO_2, so that the weight of the monoclinic

$Zr_{1-x}Mn_xO_{2-\delta}$ should be higher than that of the cubic ZrO_2 due to the replacement of oxygen vacancies by oxygen atoms. For the weight increase in the low temperature range, the oxygen concentration should increase because of the Mn^{2+} oxidization to Mn^{3+} according to the defect reaction.

Fig. 5(a) ~ (f) show the SEM fracture morphology of various dopant concentration Mn-doped zirconia samples after sintering at 1400℃and thermal etching at 1350℃. The microstructure evolution of the compacts represents clearly here. We found that for the low dopant concentration samples (lower than 10 at.%), the crystalline grains are relatively small (less than 2μm); when the dopant amount up to 15at.%, some large grains (about 20μm) are found accompanied by some small crystals surrounding along the grain boundaries; further increasing the Mn concentration, typical equiaxed grains are found and a good particle packing is reached. If the Mn concentration in ZrO_2 exceeds the solubility limit, MnO will precipitate from the solid solution. Comparing with the XRD patterns (Fig. 2), it is obvious that the grain size is small for the dual-phase structure, whereas the grains for the single cubic structure grow up very fast. The $Zr_{0.85}Mn_{0.15}O_{2-\delta}$ sample has a representative transition microstructure. In yttrium-stabilized ZrO_2 (YSZ) system, many researchers have studied the grain growth and the microstructural development [20, 21]. The grain growth rate in the cubic YSZ is faster than in the tetragonal YSZ. In our experiment, 1400℃ is high enough to make the pure monoclinic ZrO_2 transform into the tetragonal phase. With the Mn doping into ZrO_2 if the Mn concentration is sufficient to form the cubic phase, the cubic grains grow up fast, however if the Mn concentration is insufficient, the surrounding tetragonal grains will retard the cubic grain growth.

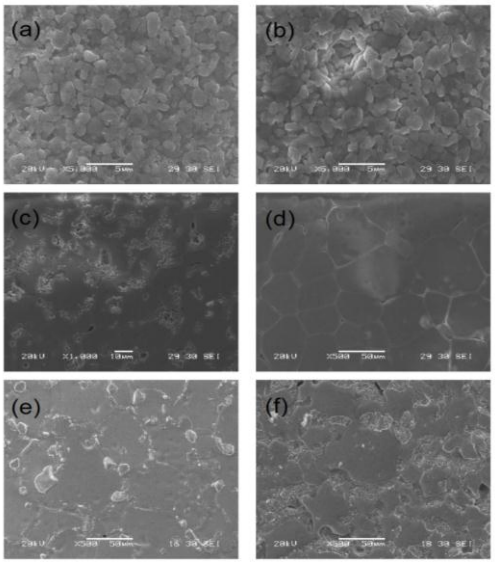

Fig. 5. SEM micrograph of $Zr_{1-x}Mn_xO_{2-\delta}$ with different dopant concentrations: (a) 5at.%; (b) 10at.%; (c) 5at.%; (d) 20at.%; (e) 25at.% and (f) 50at.%.

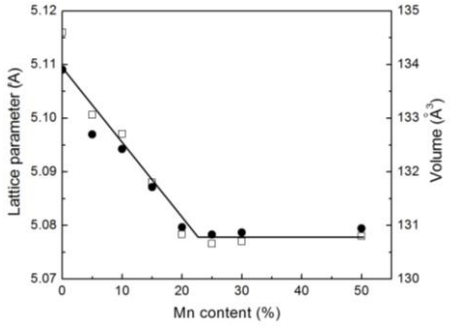

Fig. 6. Lattice parameter and cell volume for the cubic phase as a function of the Mn concentration. The round spot is guide for lattice parameter and the square is for cell volume.

From x-ray diffraction peaks, the lattice parameter was calculated with the use of FULLPRO and the solubility of Mn in cubic ZrO_2 was determined by observing the variation of the lattice parameter with increasing the Mn content. Fig. 6 illustrates the values of lattice parameter and cell volume of the cubic phase versus Mn content. A linear decrease in the lattice parameter was observed with increasing the Mn content. When the solid solubility limit is reached, the minimal lattice parameter and cell volume of the cubic phase are observed. Comparing with the results of XRD, SEM and lattice parameters, we conclude that the solubility limit of Mn in the cubic ZrO_2 is about 23at.% under our synthesis conditions.

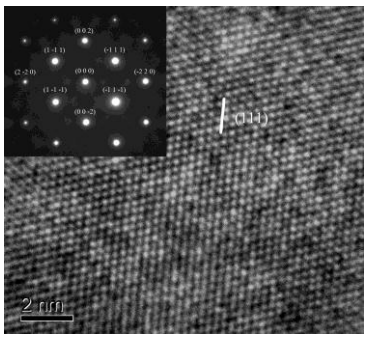

Fig. 7. HRTEM image and SAED pattern of $Zr_{0.8}Mn_{0.2}O_{2-\delta}$ along [110] direction.

Typical high resolution transmission electron microscopy (HRTEM) image and selected area electron diffraction (SAED) pattern of $Zr_{0.8}Mn_{0.2}O_{2-\delta}$ are shown in Fig. 7. The SAED pattern was taken along the [110] direction. The atoms arrange very regularly as shown in the HRTEM image and can be assigned to the corresponding cubic structure of ZrO_2. The detailed diffraction pattern of the [110] orientation is nearly the same as that of the high dopant amount of Mn in the cubic YSZ, but slightly different from that of the case of 8 mol% YSZ and the low dopant concentration [22]. It may be due to the different defect compensation mechanism or defect clustering effect.

We now discuss the structure evolution in the $Zr_{1-x}Mn_xO_{2-\delta}$ during heat treatment. There are a number of

candidate solution mechanisms for the incorporation of RO_x into ZrO_2 and each mechanism is associated with different charge compensation defects. For the MnO-ZrO_2 solid solution, the mechanisms considered in the present study are:

$$MnO \rightarrow Mn''_{Zr} + V_O^{\cdot\cdot} + O_O^{\times} \quad (1)$$

$$MnO \rightarrow Mn''_{Zr} + Mn_i^{\cdot\cdot} + O_O^{\times} \quad (2)$$

The measured density for $Zr_{0.8}Mn_{0.2}O_{1.8}$ sintered at 1400℃ is 5.605 g/cm^3 and according to the lattice parameter of the solution a = 0.508 nm, the calculated density is 5.715 g/cm^3. Comparing to the measured value, the error is smaller than 2%. We thus believe that with the Mn ions doping into ZrO_2, a substitution solid solution is formed and the vacancy compensation (Equation1) is the most favorable solution mechanism in our case.

Besides the vacancy compensation mechanism, the valence state of Mn ions is also another important effect which can cause the phase transition in the Mn-Zr-O system. For the sintering stage, MnO_2 as the initial reactive material changes into lower valence state oxides with increasing the temperature, and makes it easier to introduce oxygen vacancy into the ZrO_2 lattice. Some reporters [23] said that Mn^{3+} and Mn^{4+} ions entered the m-ZrO_2 at 1273-1623 K and Mn^{3+} and Mn^{2+} ions entered the t-ZrO_2 at 973-1173 K and at 1623 K into the cubic YSZ in air. Here we suggest that in Ar atmosphere, MnO_2 first decomposed into Mn_2O_3 at 550℃ and then into Mn_3O_4 at 800℃ (as shown in Fig. 4(a)), finally Mn^{3+} and/or Mn^{2+} have gone into m-ZrO_2 at 1100℃ due to a slight shift of the diffraction peaks of pure m-ZrO_2. When the temperature is higher than the m-t phase transition temperature (1170℃), the pure m-ZrO_2 gradually changes into the tetragonal phase; with incorporating more Mn ions into the lattices the cubic structure is stabilized.

When the synthesized cubic solution was annealed in air, the cubic to monoclinic phase transformation occurs. Comparing with the phase diagram calculated by Chen [13], 900℃ is in the range of monoclinic phases, the cubic phase is relatively stable and can not directly change into the monoclinic phase. But according to our results, if the cubic phase annealed at 900℃ in air, a little of the monoclinic phase could be found. A possible explanation is that at this temperature range, the initial Mn^{2+} in the cubic solution was oxidized into Mn^{3+}, which resulted in the reduce of the oxygen vacancy concentration. On the other hand, due to the difference of ionic radii between Mn^{2+} and Mn^{3+}, the smaller Mn^{3+} causes a larger lattice distortion and makes the cubic structure unstable.

4. Conclusion

In search for the structure evolution and stabilization mechanism, a zirconia doped with up to 50at.% manganese was synthesized by solid solution reaction. The maximum solubility of Mn in the cubic ZrO_2 is 23at.% and the grain growth of the single-phase solution is much faster than that of the dual-phase materials. Oxygen vacancy is one of the most important effects which can make the high symmetry structure retain to room temperature. Cubic to monoclinic phase transformation is driven by the decrease of the oxygen vacancy quantity and the modification of the valence state of Mn ions.

Acknowledgments

This work was financially supported by the National Science Fund Program of China (Grant No. 50872115).

References

[1] H. G. Scott, J. Mater. Sci. **10**, 1527 (1975).
[2] R. M. Dickerson, M. V. Swain, A. H. Hwuer, J. Am. Ceram. Soc. **70**, 214 (1987).
[3] D. Viechnicki, V. S. Stubican, J. Am. Ceram. Soc. **48**, 292 (1965).
[4] S. Ostanin, A. Ernst, L. M. Sandratskii, P. Bruno, M. D˙.ane, I. D. Hughes, J. B. Staunton, W. Hergert, I. Mertig, J. Kudrnovsk´y, Phys. Rev. Lett. **98**, 016101 (2007).
[5] A. Keshavaraja, A. V. Ramaswamy, J. Mater. Res. **9**, 837 (1994).
[6] V. R. Choudhary, B. S. Uphade, S. G. Pataskar, A. Keshavraja, Angew, Chem. Int. Ed. Engl. **35**, 2393 (1996).
[7] K. Eguchi, M. Watabe, S. Ogata, H. Arai, Bull. Chem. Soc. Jpn. **68**, 1739 (1995).
[8] M. Hino, S. Kobayashi, K. Arata, J. Am. Chem. Soc. **101**, 6439 (1979).
[9] K. T. Jung, A. T. Bell, J. Mole. Ctatl. A: Chem **163**, 27 (2000).
[10] J. Yu, L. B. Duan, Y. C. Wang, G. H. Rao, Physica B **403**, 4264 (2008).
[11] G. Clavel, M G. Willinger, D. Zitoun, N. pinna, Eur. J. Inorg. Chem. 2008, 863 (2008).
[12] A. Pucci, G. Clavel, M G.Willinger, D. Zitoun, N. Pinna, J. Phys. Chem. C **113**, 12048 (2009).
[13] M. Chen, B. Hallstedt, Ludwig J. Gauckler, Solid State Ionics **176**, 1457 (2005).
[14] G. Bayer, J. Am. Ceram. Soc. **53**, 294 (1971).
[15] A. Nicholas Grundy, B. Hallstedt, L. J. Hauckler, J. Phase Equilibria **24**, 21 (2002).
[16] H. F. McMurdie, E. Golovato, J. Res. Natl. Bur. Stand. **41**, 589 (1948).
[17] C. Klingsberg, R.Roy, J. Am. Ceram. Soc. **48**, 620 (1960).
[18] H. E. Kissinger, H. F. McMurdie, B. S. Simpson, J. Am. Ceram. Soc. **39**, 168 (1956).
[19] L. Gao, L. Zhou, J. Q. Feng, L. F. Bai, C. S. Li, Z. Y. Liu, J. L. Soubeyroux, Y. F. Lu, OI:10.1016/j.ceramint.2011.10.082. (2011).
[20] K. Matsui, H. Yoshida, Y. Ikuhala, Acta Mater. **56**, 1315 (2008).
[21] Y. Yoshizawa, T. Sakuma, ISIJ Int. **29**, 746 (1989)
[22] C. C. Appel, G. A. Botton, A. Horsewell, W. Michael Stobbs, J. Am. Ceram. Soc. **82**, 429 (1999).
[23] M. Occhiuzzi, D. Cordischi, R. Dragone, Phys. Chem. Chem. Phys. **5**, 4938 (2003).

*Corresponding author: yflu@c-nin.com